

Effect of Homogeneity on Microstructure, Dielectric, and Ferroelectric Properties of Strontium Barium Niobate

P.K. Patro¹, A.R. Kulkarni¹, S.M. Gupta², and C.S. Harendranath¹

¹Indian Institute of Technology Bombay, Mumbai-400 076

²Centre of Advanced Technology, Indore-452 013

ABSTRACT

Strontium barium niobate (SBN) is tetragonal tungsten bronze structured ferroelectric material. It is one of the few lead-free ferroelectrics in the fore-front of environment-friendly electroceramic research and development. The unusual sintering behaviour of SBN exhibits abnormal grain growth, duplex microstructure, and low density that has plagued commercial exploitation of SBN. The formation of duplex microstructure becomes more prominent when synthesised by conventional solid-state approach. Compositional inhomogeneity is believed to be the key player of such ambiguity. Will homogeneous mixing eliminate this problem? To answer this question, first SBN was synthesised by conventional solid-state technique, then coprecipitation technique, a wet chemical route, was employed for synthesis of SBN. In coprecipitate route, the precursors were mixed at the molecular level. It is thought that the improved composition uniformity might help in eliminating microstructure-related problems with improved dielectric properties. The findings in this connection on microstructure, dielectric, and ferroelectric properties of SBN when synthesised by conventional solid-state route as well as coprecipitation route have been discussed.

Keywords: Strontium barium niobate, SBN, lead-free ferroelectrics, solid-state technique, coprecipitate technique, dielectric properties, ferroelectric properties, homogeneity, microstructure

1. INTRODUCTION

Strontium barium niobate ($Sr_xBa_{1-x}Nb_2O_6$, $0.25 \leq x \leq 0.75$, abbreviated as SBN) is a promising lead-free ferroelectric-based material, owing to its large pyroelectric¹, electro-optic², nonlinear optical properties³, etc. The physical and electrical properties vary with composition and sintering conditions. Although single crystal of SBN with varying composition has been used immensely, it finds restricted application because of difficulty in fabrication and associated high cost. For optical applications, it is desirable that SBN should have a density near to theoretical one and uniform microstructure. But SBN ceramic,

with nearly-theoretical density, is difficult to obtain during pressureless sintering because of abnormal grain growth⁴. Efforts have been made to obtain high density SBN by hot pressing⁵, double-stage sintering⁴, and using sintering aids⁶. Alternate synthesis methods such as partial coprecipitation⁷, coprecipitation⁸, solution combustion⁹, sol-gel¹⁰, EDTA-complex chemical method¹¹, etc have also been employed to improve its physical, dielectric, and microstructural properties.

In this study, the conventional solid-state synthesis method and coprecipitation method—the wet chemical route have been adopted to explain the effect of

homogeneity in the precursors and their consequence on the microstructural, dielectric, and ferroelectric properties of SBN.

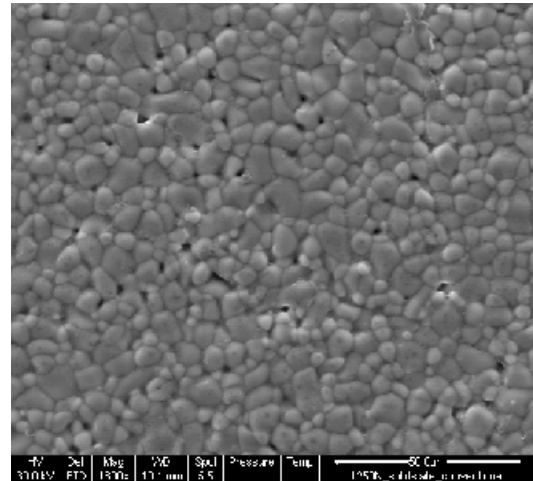
2. EXPERIMENTAL PROCEDURE

The precursors used for synthesis of SBN by solid-state method as well as coprecipitation method were Nb_2O_5 (99.99 %), $Sr(NO_3)_2$ (99 %), $Ba(NO_3)_2$ (99 %) and $NbCl_5$ (99 %) procured from Aldrich, USA. For both syntheses, the detailed experimental procedure followed are discussed elsewhere^{9,13}. The pure powder thus obtained by the above synthesis method was pelletised and sintered at different temperatures (from 1250 °C to 1350 °C). The sintered pellets were subjected to microstructural, dielectric, and ferroelectric characterisation. For simplicity, the pellets sintered at 1250 °C, 1300 °C, and 1350 °C are abbreviated as SN1250, SN1300 and SN1350 in the solid-state synthesis method and similarly for coprecipitation method abbreviated as CPAH1250, CPAH1300, and CPAH1350.

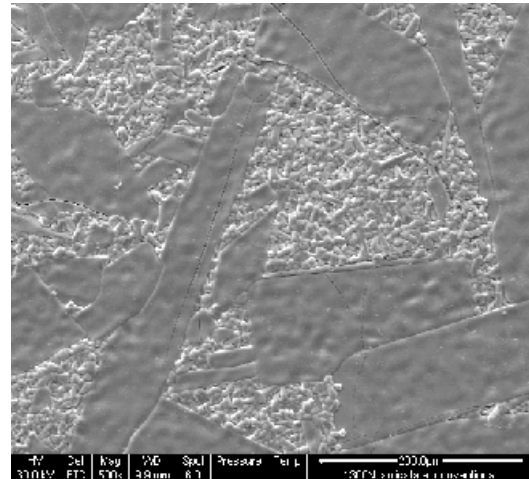
3. RESULTS

X-ray diffraction of the calcined powder showed the presence of pure SBN50 ($Sr_{0.5}Ba_{0.5}Nb_2O_6$) phase after the calcination temperature of 1150 °C for both the sets of samples. The tunneling electron micrograph (TEM) showed the particle size of the calcined powder (1150 °C) having the pure SBN50 phase to be in the range ~250 nm for the powder synthesised by conventional solid-state method, whereas it was 100-250 nm for coprecipitation method.

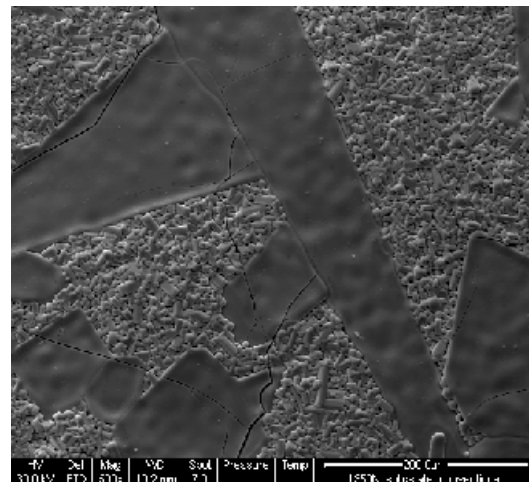
The scanning electron micrograph (SEM) of the sintered pellets is shown in Figs 1(a), 1(b), and 1(c) and Figs 2(a), 2(b) and 2(c) for solid-state and coprecipitation-based samples corresponding to the sintering temperature of 1250 °C, 1300 °C, and 1350 °C, respectively. The micrograph corresponding to SN1250 [Fig. 1(a)] shows that the grains are of the order of 7 m. The micrograph corresponding to SN1300 [Fig. 1(b)] shows two types of grains. One is small sized, elongated grains of the range 10-15 m and the other type is very large, and ranges between 50-150 m. This grain seems to be very thin and almost transparent in nature so that



(a)

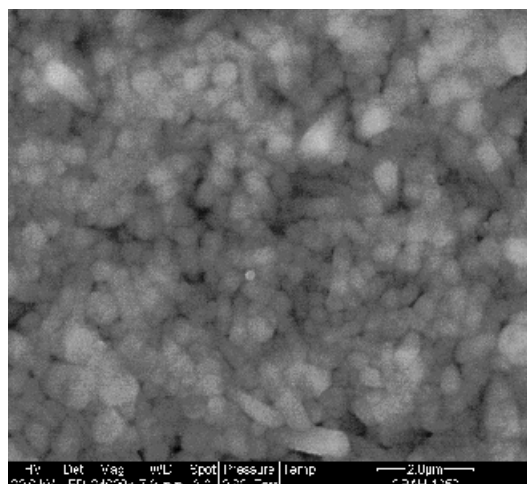


(b)

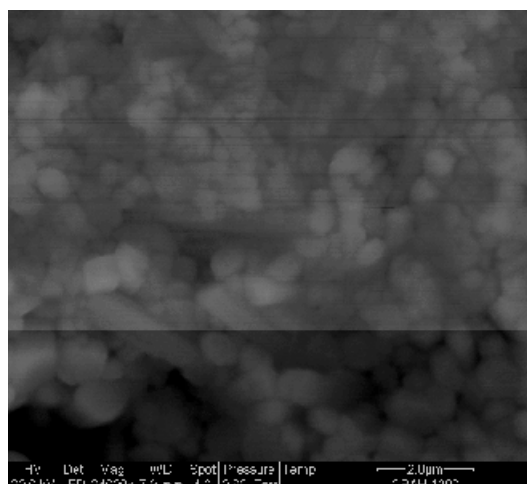


(c)

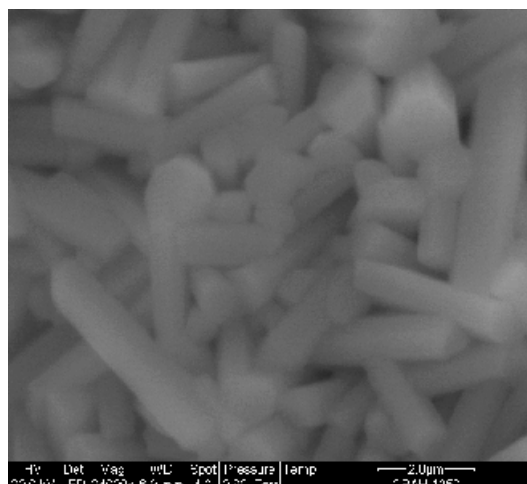
Figure 1. SEM of sintered pellets of SBN50 synthesised by solid-state method: (a) SN1250, (b) SN1300, and (c) SN1350.



(a)



(b)



(c)

Figure 2. SEM of sintered pellets of SBN50 synthesised by coprecipitate method: (a) CPAH1250, (b) CPAH1300, and (c) CPAH1350.

the presence of smaller grains (of type one) can be seen. Figure 1(c) corresponding to SEM of SN1350 again shows the presence of duplex microstructure with two types of grains. The smaller grains in the micrograph are more or less rectangular in shape and also show the presence of micro-cracks. For this sintering temperature, the bigger grains now have become of order of 200 m.

Figures 2(a), 2(b), and 2(c) show the SEM of the CPAH1250, CPAH1300, and CPAH1350 samples. The micrographs show uniformity in the grain size. Figure 2(a), corresponding to CPAH1250, shows some pores, showing that the pellet is not very well sintered. Figure 2(b) shows that the sample is well sintered having uniform grains. A very few number of grains with a tendency of uniaxial grain growth were also seen. A large number of uniaxial micro-rod shaped grains were seen in the case of CPAH1350 [Fig. 2(c)]. This may be due to Ostwald ripening of grains, where the bigger grains grow at the expense of smaller grains. The image analyses of the micrographs revealed that the mean grain sizes were 0.70 m, 0.78 m, and 3.46 m and aspect ratios were 1.34, 1.54, and 3.46 for CPAH1250, CPAH1300, and CPAH1350, respectively.

4. DISCUSSIONS

From the above results it is clear that there is a striking dissimilarity in the grain morphology when the synthesis methods were different. The former (by solid-state method) resulted in a duplex microstructure with abnormal grain growth and micro-cracks. The latter (by coprecipitate method) resulted in a uniform microstructure with no abnormal grain growth. At the sintering temperature of 1350 °C, however some small and elongated grains were observed in the micrographs. This microstructural difference is liked to be reflected on the dielectric and ferroelectric properties, discussed subsequently.

The dielectric properties of the sintered pellets were measured from -50 °C till 200 °C, using a high- resolution dielectric analyser with standard internal reference. The measurement was done from 100 Hz to 1 MHz in the heating cycle (Novocontrol Alpha Analyser and Solartron SI1260 Impedance Analyser). The porosity-corrected dielectric constant¹³

versus temperature plot for poled solid-state-based and coprecipitation-based samples for the sintering temperatures of 1250 °C, 1300 °C, and 1350 °C are shown in Figs 3(a), 3(b), and 3(c) and Figs 4(a), 4(b), and 4(c), respectively. The broad dielectric peak indicates the second-order phase transformation, i.e., characteristics of relaxor ferroelectrics. But the shift of ferroelectric-paraelectric phase-transition temperature, T_m with frequency is not very prominent for the solid-state-based samples whereas it is clearly visible for the coprecipitation-based samples.

Figure 3(a), corresponding to SN1250 shows a very low ϵ'_{\max} value (535). With increase in the sintering temperatures, the ϵ'_{\max} increased to 897 and 1428 for SN1300 and SN1350 respectively. Interestingly, values of T_m were found to be varying with sintering temperature. T_m values were found to be 110 °C, 120 °C, and 130 °C for SN1250, SN1300, and SN1350, respectively. The change of

T_m with sintering temperature may be dependent upon the stress in the samples. Higher the stress, the lower is the T_m . In the present cases, the SEM shows that with increase in sintering temperature, it results in a duplex microstructure with abnormal grain growth and micro-cracks. These micro-cracks helped in releasing the stress due to abnormal grain growth, and hence in turn, increased T_m values¹².

For CPAH1250, CPAH1300, and CPAH1350, ϵ'_{\max} were 2717, 2847, and 3281, respectively. Similarly ϵ'_{RT} (dielectric constant at room temperature) was 2327, 2779, and 2643, respectively [Figs 4(a), 4(b), and 4(c)]. T_m was found to be 47 °C, 57 °C, and 60 °C for CPAH1250, CPAH1300, and CPAH1350, respectively for 1 kHz frequency.

It can be clearly seen that there is a notable difference in the dielectric properties of SBN, when processed through two different routes. SBN, synthesised

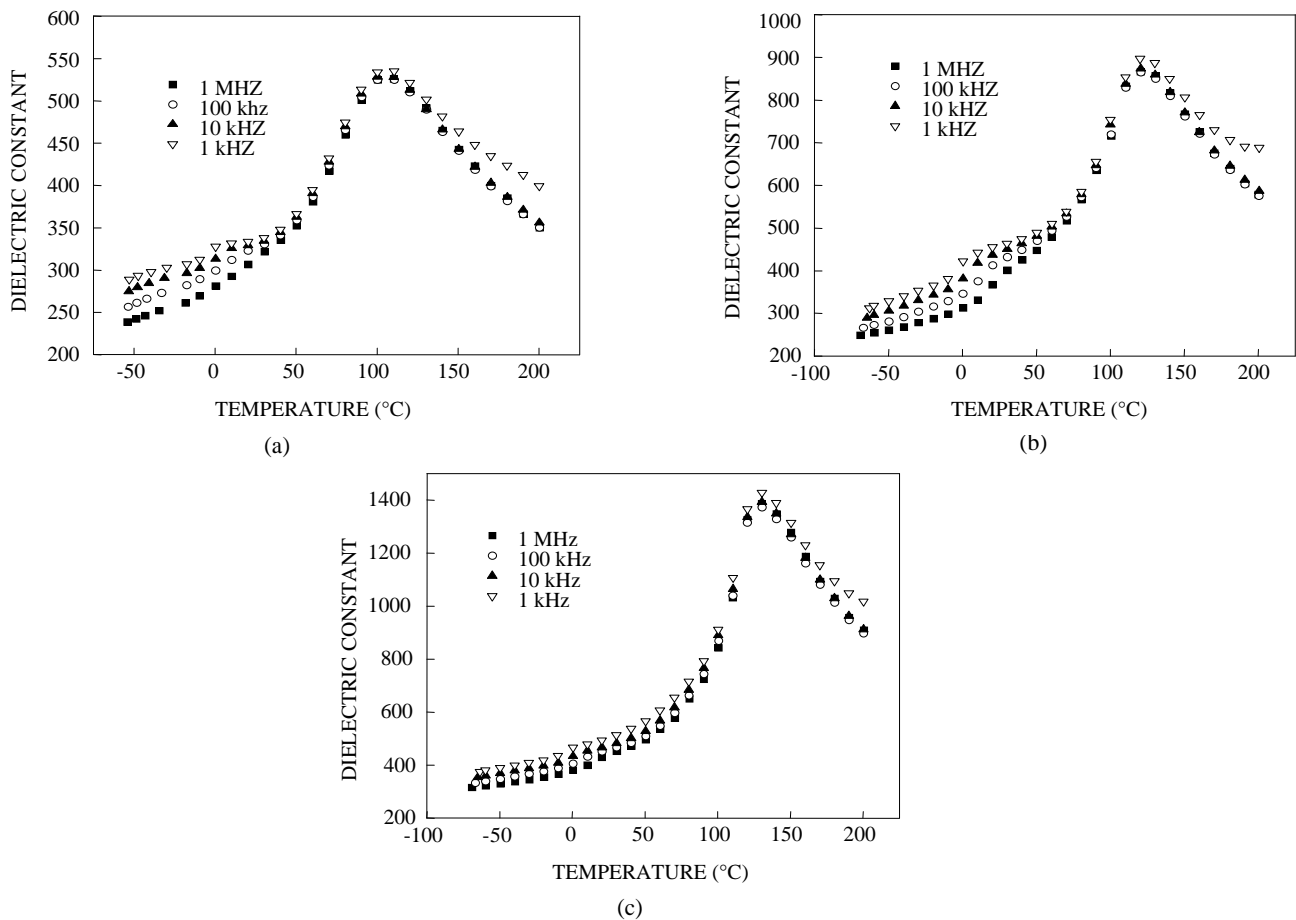


Figure 3. Variation of dielectric constant against temperature for sintered pellets of SBN50 synthesised by conventional solid-state method: (a) SN1250, (b) SN1300, and (c) SN1350.

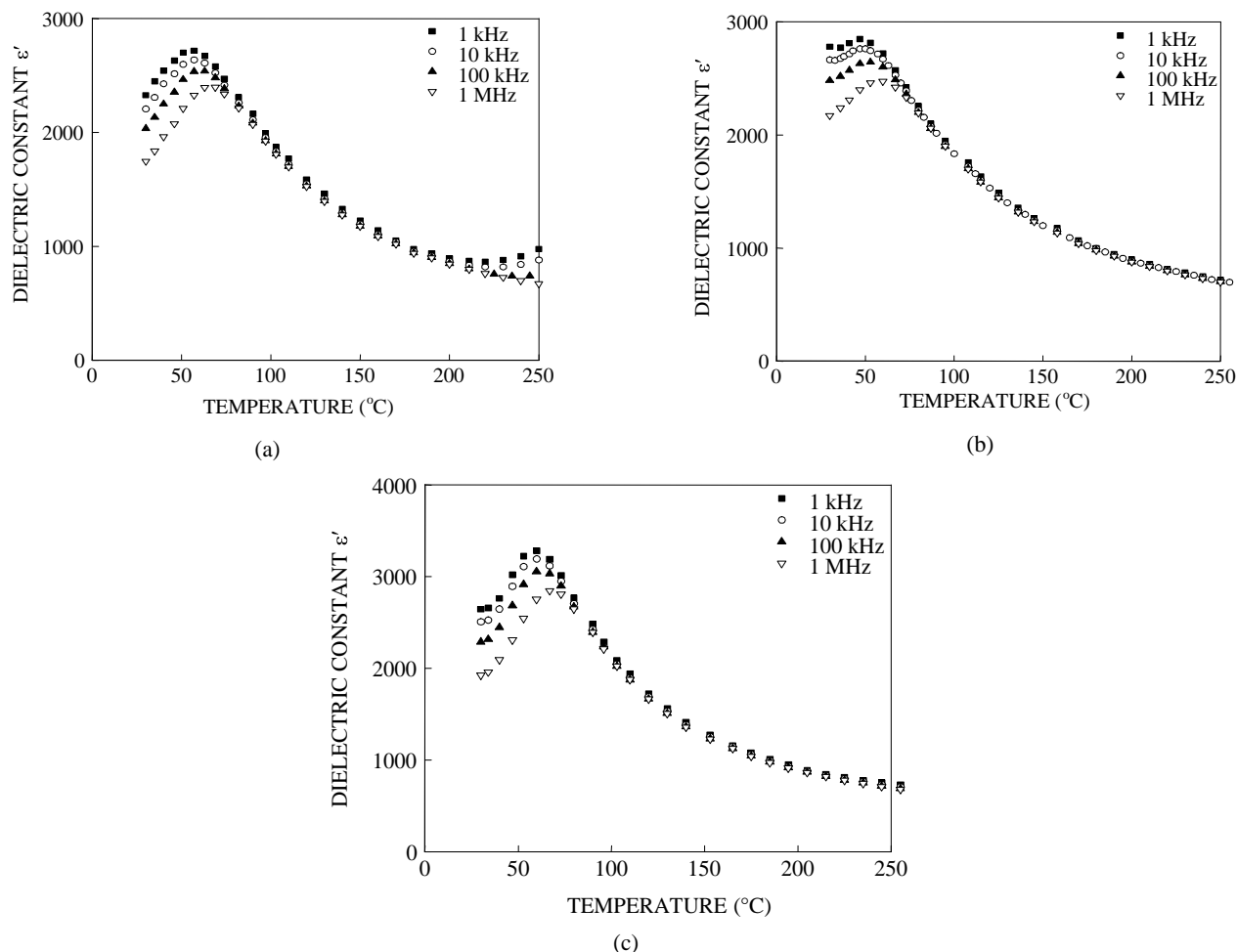
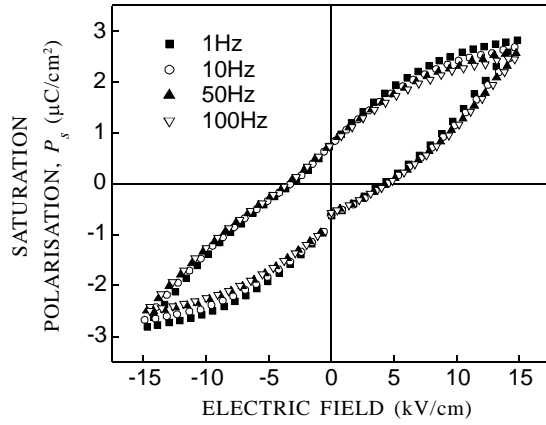


Figure 4. Variation of dielectric constant against temperature for sintered pellets of SBN50 synthesised by coprecipitate method: (a) CPAH1250, (b) CPAH1300, and (c) CPAH1350.

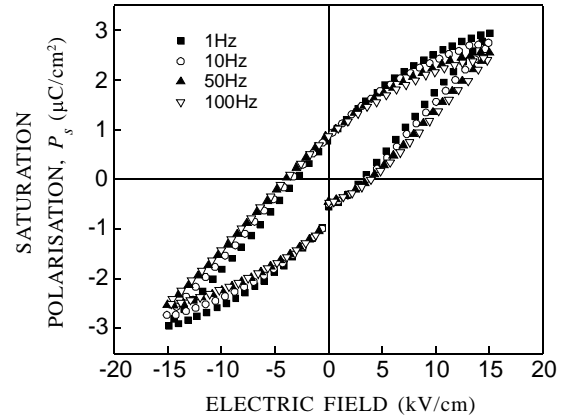
by coprecipitate method resulted in a material with the dielectric properties superior to those synthesised by conventional solid-state route. The room temperature dielectric constants (T_R) for the coprecipitation-synthesised are significantly higher than the conventionally-processed SBN.

The ferroelectric hysteresis loop at an electric field of 15 kV/cm at different frequencies (Radiant Technology Precision Workstation) for the samples are shown in the Figs 5(a), 5(b), and 5(c), and Figs 6(a), 6(b), and 6(c) for conventional solid-state method and coprecipitation method synthesised SBN respectively. It can be clearly seen that for the solid-state-processed sample, the highest polarisation was observed for SN1250. However, saturation polarisation (P_s) values decreased with increase in sintering temperatures in samples synthesised by

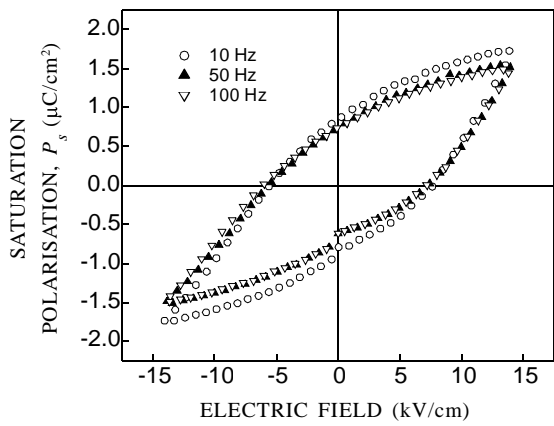
solid-state method. The decrease in ferroelectric properties can be attributed to the duplex microstructure with abnormal grain growth. The effect of abnormal grain growth, which was not of much significance on the dielectric properties, played a major role in decreasing the ferroelectric properties of SBN. It can also be noted that, the P-E data could not be acquired for 1 Hz frequency, because of lossy nature of the material. For SBN Synthesised by coprecipitation P-E method, non-lossy P-E loops were obtained [Figs 6(a), 6(b), and 6(c)],mn. For 1 Hz frequency, the maximum saturation polarisation observed for CPAH1350 was $5.6 \mu\text{C}/\text{cm}^2$. Similarly, the saturation polarisation (P_s) of CPAH1250 and CPAH1300 were $2.93 \mu\text{C}/\text{cm}^2$ and $4.03 \mu\text{C}/\text{cm}^2$ for 1 Hz frequency respectively. It is quite clear that



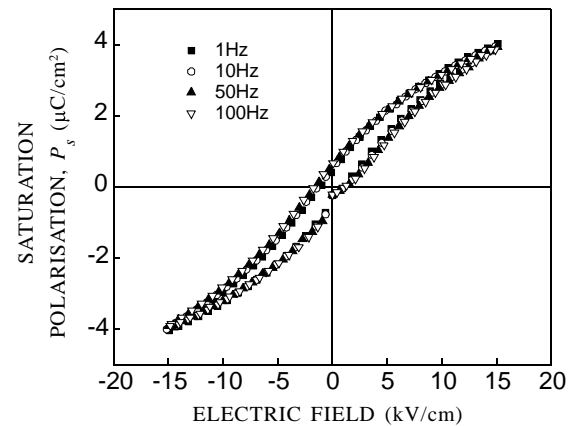
(a)



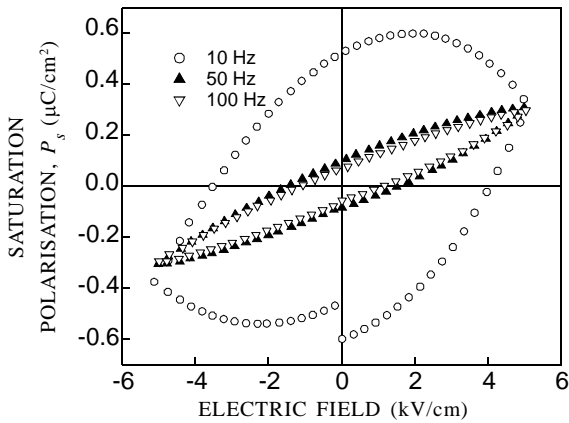
(a)



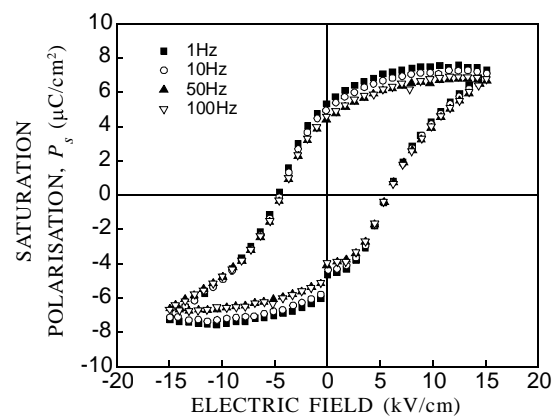
(b)



(b)



(c)



(c)

Figure 5. Ferroelectric hysteresis loop of SBN50 synthesised by solid-state route: (a) SN1250, (b) SN1300, and (c) SN1350, at different frequencies.

Figure 6. Ferroelectric hysteresis loop of SBN50 synthesised by coprecipitate route: (a) CPAH1250, (b) CPAH1300, and (c) CPAH1350 at different frequencies.

SBN by coprecipitate synthesis method resulted in a material with better ferroelectric properties and has non-lossy nature.

Keeping in mind the analogy with magnetisation behaviour in superparamagnetic materials, the polarisation behaviour of an ensemble of uniform

non-interacting polar clusters, having uniaxial symmetry, can be described by Neel's equation¹⁴. Therefore, it is expected that superparaelectric behaviour is analogous to superparamagnetic behaviour in ferroelectrics. It follows that if reduced polarisation (P) at different specific temperatures, T is plotted against E/T (rather than B , as in superparamagnetics), all the curves should superimpose on each other. Observation of such a master curve would imply that the clusters are indeed non-interacting in nature. In the present study on coprecipitated SBN, Fig. 7(a) is the plot of reduced temperatures under considerations are in the paraelectric range as Neel's law is only valid for paraelectric regions. These clearly show that the curve is not superimposing. On the other hand, this shows that there are no non-interacting polar clusters. However, when the

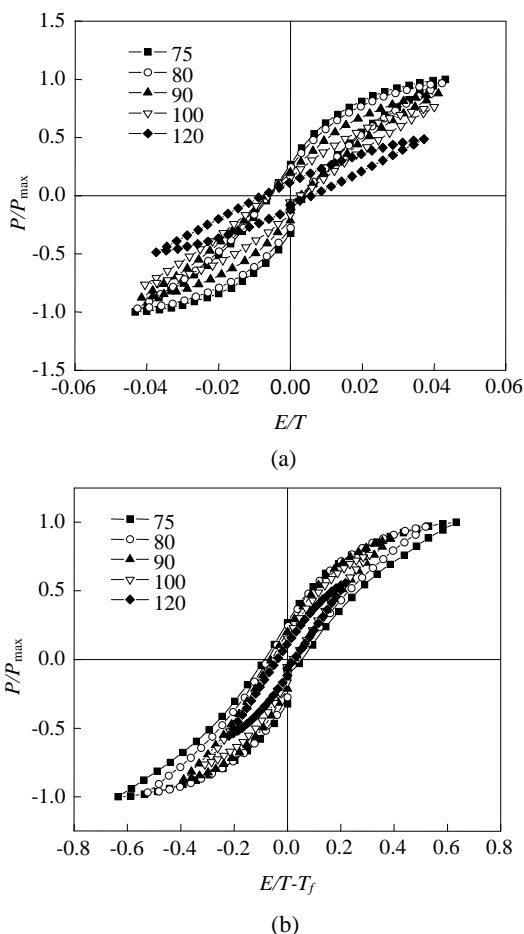


Figure 7. Variation of reduced polarisation P_s : (a) with normalised electric field (Neel's law) and (b) with reduced normalised electric field of SBN50 synthesised by coprecipitate method (modified Neel's law).

normalised polarisation (P) is plotted against $E/(T-T_f)$, the curves at different temperatures (again only the paraelectric temperatures) almost superimpose. This is shown in Fig. 7(b). This indicates that the reduced polarisation (P_s) follows modified Neel's equation in which an extra parameter (T_f) is introduced. In conclusion, a non-zero interaction among the polar clusters is implied.

In addition, other ferroelectric characterisations like current-voltage (I-V), leakage and fatigue characteristics were studied. Here, results corresponding to the sintering temperature 1350 °C (SN1350 and CPAH1350) are only summarised. Figure 8 depicts the current-voltage (I-V) characteristics of the samples under consideration. A switched triangular profile is used where, in first stage, the voltage rises from zero to a value V_{max} in steps, and then drops back to zero with the same number of steps. In the second stage, a negative V_{max} is applied following the same steps as mentioned above. The leakage current varied from 10^{-5} A to 10^{-11} A in solid-state-synthesised SBN, whereas it varied from 10^{-6} to 10^{-11} A for the coprecipitate synthesised SBN. The hysteresis in the curve shows the charge storage nature of ferroelectrics. The leakage current tests are done on the samples at the applied electric field of 15 kV/cm at the soaking time and the measurement time of 1000 ms. Leakage current of the order of 10^{-5} A is observed for solid-state synthesised SBN sample whereas it is of the order of 10^{-6} for coprecipitate synthesised SBN sample (Fig. 9).

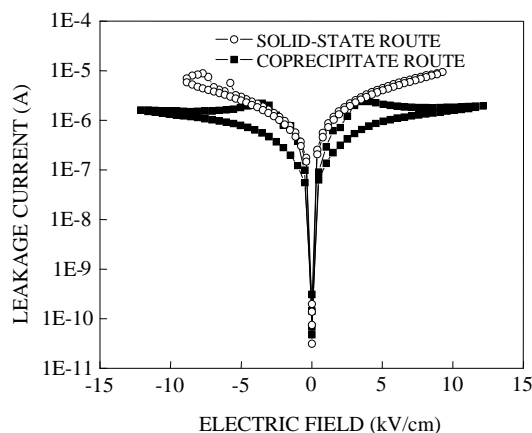


Figure 8. Current-voltage (I-V) plot of SBN50 synthesised by coprecipitate method and solid-state method.

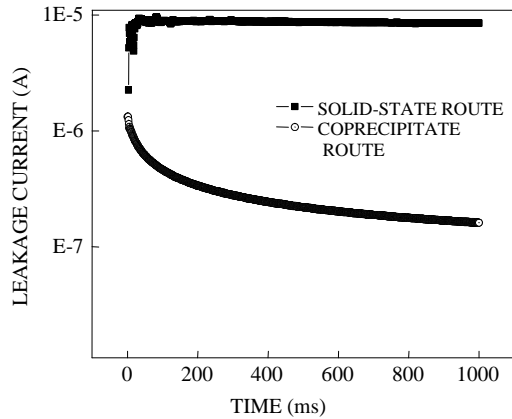


Figure 9. Leakage current plot of SBN50 synthesised by coprecipitate route and solid-state route.

It can also be seen from the figure that, leakage current is constant over the measurement time period in the solid-state-synthesised SBN whereas it decreases with time in the coprecipitated-synthesised SBN. The electric cycling fatigue test was conducted on both the samples at the electric field of 15 kV/cm and at 500 Hz. The resulting change in polarisation at different time intervals was measured. Figure 10 shows the fatigue behaviour of the samples where plot is of saturation polarisation (P_s) versus number of electric cycles at constant electric field. This clearly shows that all the samples are quite stable on repeated application of electric field. In the coprecipitated sample, which has a high P_s value, shows a tendency of decrease in it over the number of electric cycling fatigue measurement. However, this change is very small when compared to the number of electric cycles applied (Fig. 10).

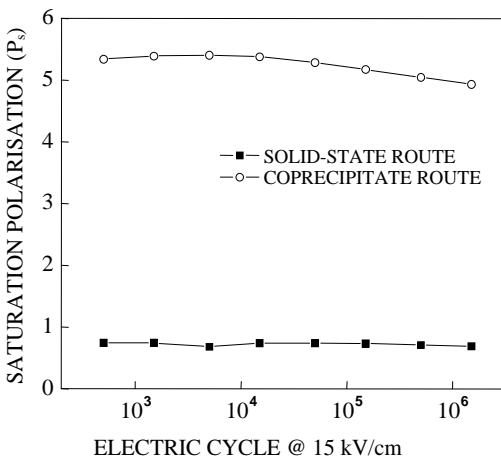


Figure 10. Fatigue characteristics of SBN50 synthesised by coprecipitate route and solid-state route.

4. CONCLUSION

The SBN synthesised by coprecipitation method not only resulted in uniform microstructure with no abnormal grain growth but also with remarkably improved dielectric and ferroelectric properties. It also showed the relaxor behaviour, followed $V-F$ relationship indicating dipolar-glass nature, low time induced as well as field-induced leakage current, superior electric fatigue resistance properties, and above all, T_m value close to room temperature. All these properties make SBN synthesised by coprecipitation method a better choice for device applications than the material synthesised by the conventional solid-state route.

ACKNOWLEDGEMENT

The authors acknowledge Sophisticated Analytical Instrument Facility (SAIF), IIT Bombay, Mumbai, for TEM and SEM studies. They also acknowledges CSIR for the Senior Research Fellowship Grant.

REFERENCES

1. Glass, A.M. Investigation of electrical properties of $Sr_{1-x}Ba_xNb_2O_6$ with special reference to pyroelectric detection. *J. Appl. Phys.*, 1969, **40**(12), 4699-713.
2. Liu, S.T.; Maciolek, R.B.; Zook, J.D. & Rajagopalan, B. Electrooptic and ferroelectric effect in La -doped SBN single crystals. *Ferroelectrics*, 1988, **87**, 265-69.
3. Xu, Y.; Chen, H.C. & Liu, S.T. Optical properties and linear electrooptic effect in ferroelectric single crystal KNSBN. *Jpn. J. Appl. Phys.*, 1985, **24**, 278-80.
4. VanDamme, N.S.; Sutherland, A.E.; Jones, L.; Bridger, K. & Winzer, S.R. Fabrication of optically transparent and electro-optic strontium barium niobate ceramics. *J. Am. Ceram. Soc.*, 1994, **74**(8), 1785-792.
5. Nagata, K.; Yamamoto, Y.; Igarashi, H. & Okazaki, K. Properties of the hot-pressed strontium barium niobate ceramics. *Ferroelectrics*, 1981, **38**, 853-56.
6. Lee, S.I. & Choo, W.K. Modified ferroelectric high density strontium barium niobate ceramics

for pyroelectric applications. *Ferroelectrics*, 1988, **87**, 209-12.

7. Patro, P.K.; Kulkarni, A.R. & Harendranath, C.S. Microstructure and dielectric properties of strontium barium niobate ceramic, synthesised using partial coprecipitation. *J. Euro. Ceram. Soc.*, 2003, **23**(8), 1329-335.
8. Patro, P.K.; Kulkarni, A.R. & Harendranath, C.S. Combustion synthesis of $Sr_{0.5}Ba_{0.5}Nb_2O_6$ and effect of fuel on its microstructure and dielectric properties. *Mater. Res. Bull.*, 2003, **38**(2), 249-59.
9. Patro, P.K.; Deshmukh, R.D.; Kulkarni, AR.; & Harendranath, C.S. Synthesis of $Sr_{0.5}Ba_{0.5}Nb_2O_6$ by coprecipitation method-dielectric and microstructural characteristics. *Journal Electroceramics*, 2004, **13**(3), 479-85.
10. Hirano, S.; Yogo, T.; Kikuta, K. & Ogiso, K. Preparation of strontium barium niobate by sol-gel method. *J. Am. Ceram. Soc.*, 1992, **75**(6), 1697-700.
11. Panda, A.B.; Pathak, A. & Pramanik, P. Low temperature preparation of nanocrystalline solid solution of strontium-barium-niobate by chemical process. *Material Letters*, 2002, **52**(3), 180-86.
12. Rushman, D.F. & Strivens, M.A. The effective permittivity of two-phase system. *Proc. Phys. Soc.*, 1947, **59**, 1011-016.
13. Patro, P.K.; Kulkarni, A.R. & Harendranath, C.S. Dielectric and ferroelectric behavior of SBN50 synthesized by solid-state route using different precursors. *Ceramic International*, 2004, **30**(7), 1405-409.

Contributor



Dr P.K. Patro obtained his MSc (Chemistry) from the Berhampur University, Orissa, and PhD (Electroceramics) from the Dept of Metallurgical Engineering and Materials Science, IIT Bombay, Mumbai. He joined Bhabha Atomic Research Centre (BARC), Mumbai, as a Dr KS Krishnan Research Associate (KSKRA). He is recipient of *Best Technical Paper Award* in International Symposium for Research Students - 2004 (ISRS04) held at IIT Madras, Chennai. At present, he is involved in the solid oxide fuel cell development activities. His research interests include: Advanced ceramic processing, electron microscopy, impedance spectroscopy of ferroelectrics/piezoelectrics and solid-state ionics.